Intelligent Robots and Computer Vision X: Neural, Biological, and 3-D Methods

PROCEEDINGS
SPIE—The International Society for Optical Engineering

Intelligent Robots and Computer Vision X: Neural, Biological, and 3-D Methods

David P. Casasent
Chair/Editor

14–15 November 1991
Boston, Massachusetts

Sponsored and Published by
SPIE—The International Society for Optical Engineering

Volume 1608

Please use the following format to cite material from this book:
Author(s), "Title of paper," *Intelligent Robots and Computer Vision X: Neural, Biological, and 3-D Methods,* David P. Casasent, Editor, Proc. SPIE 1608, page numbers (1992).

Library of Congress Catalog Card No. 91-67604
ISBN 0-8194-0745-3

Published by
SPIE—The International Society for Optical Engineering
P.O. Box 10, Bellingham, Washington 98227-0010 USA
Telephone 206/676-3290 (Pacific Time) • Fax 206/647-1445

Printed in the United States of America.

CONFERENCE COMMITTEE

Conference Chair

David P. Casasent, Carnegie Mellon University

Program Committee

Mongi A. Abidi, University of Tennessee/Knoxville
Rolf-Jürgen Ahlers, Rauschenberger Group (FRG)
Bruce G. Batchelor, University of Wales College of Cardiff (UK)
Madan M. Gupta, University of Saskatchewan (Canada)
Prasanna G. Mulgaonkar, SRI International
Daniel Raviv, Florida Atlantic University
Steven K. Rogers, Air Force Institute of Technology
Matthew A. Turk, Media Laboratory/MIT

Session Chairs

Session 1—Reconstruction, Description, and Modeling of 3-D Surfaces I
Daniel Raviv, Florida Atlantic University

Session 2—Reconstruction, Description, and Modeling of 3-D Surfaces II
Prasanna G. Mulgaonkar, SRI International

Session 3—Neuromorphology of Biological Vision: A Basis for Machine Vision I
Madan M. Gupta, University of Saskatchewan (Canada)

Session 4—Neuromorphology of Biological Vision: A Basis for Machine Vision II
Madan M. Gupta, University of Saskatchewan (Canada)

Session 5—Three-Dimensional Scene Perception I
Mongi A. Abidi, University of Tennessee/Knoxville

Session 6—Three-Dimensional Scene Perception II
Mongi A. Abidi, University of Tennessee/Knoxville

Session 7—Neural Nets for Computer Vision and Intelligent Robots I
Steven K. Rogers, Air Force Institute of Technology

Session 8—Neural Nets for Computer Vision and Intelligent Robots II
Steven K. Rogers, Air Force Institute of Technology

Conference 1608, *Intelligent Robots and Computer Vision X: Neural, Biological, and 3-D Methods,* was part of a four-conference program on Computer Vision held at SPIE's Symposium on Advances in Intelligent Robotic Systems, 10-15 November 1991, in Boston, Massachusetts. The other conferences were:

Conference 1607, *Intelligent Robots and Computer Vision X: Algorithms and Techniques*
Conference 1609, *Model-Based Vision Development and Tools*
Conference 1610, *Curves and Surfaces in Computer Vision and Graphics II*

INTELLIGENT ROBOTS AND COMPUTER VISION X:
NEURAL, BIOLOGICAL, AND 3-D METHODS

Volume 1608

INTRODUCTION

This conference is intended to reflect the newest research results, trends, and developments in intelligent robots and computer vision. The emphasis in this portion of the tenth conference in this series is neural, biological, and 3-D methods. See Volume 1607 for technical papers on algorithms and techniques for intelligent robots and computer vision.

Over fifty papers from ten different countries are included, representing the truly international flavoring of this volume. The eight sessions of this conference address these three aspects of intelligent robot and computer vision systems. Sessions 1 and 2 concern the reconstruction and modeling aspects of 3-D sensors. Sessions 5 and 6 complement this with attention to 3-D scene perception using ranging and stereo 3-D sensors.

Sessions 3 and 4 concern the biological vision aspects of machine vision, while Sessions 7 and 8 contain a large set of neural net computer vision and robotics papers.

I thank my administrative assistant (Marlene Layton), and my program committee, plus all session chairs and authors who made this conference the success it was and my job more enjoyable.

David Casasent
Carnegie Mellon University

INTELLIGENT ROBOTS AND COMPUTER VISION X:
NEURAL, BIOLOGICAL, AND 3-D METHODS

Volume 1608

CONTENTS

(continued)

INTELLIGENT ROBOTS AND COMPUTER VISION X:
NEURAL, BIOLOGICAL, AND 3-D METHODS

Volume 1608

INTELLIGENT ROBOTS AND COMPUTER VISION X:
NEURAL, BIOLOGICAL, AND 3-D METHODS

Volume 1608

SESSION 1

Reconstruction, Description, and Modeling of 3-D Surfaces I

Chair
Daniel Raviv
Florida Atlantic University

A "NON-RECONSTRUCTION" APPROACH FOR ROAD FOLLOWING

Daniel Raviv* and Martin Herman**

*Robotics Center and Electrical Engineering Department
Florida Atlantic University, Boca Raton, FL 33431; and
Sensory Intelligence Group, Robot Systems Division
National Institute of Standards and Technology
Gaithersburg, MD 20899
**Sensory Intelligence Group, Robot Systems Division
National Institute of Standards and Technology
Gaithersburg, MD 20899

ABSTRACT

This paper presents a new approach for vision-based autonomous road following. By building on a recently developed optical-flow-based theory, we suggest that motion commands can be generated directly from a visual feature, or cue, consisting of the projection into the image of the tangent point on the edge of the road, along with the optical flow of this point. Using this visual cue, there is no need to reconstruct the 3-D scene, and the related computations are relatively simple. We suggest some vision-based partial control algorithms for both circular and non-circular roads.

1. INTRODUCTION

Algorithms for vision-based road following have recently been explored by many investigators [2, 3, 4, 8, 9, 10]. Most of them convert the information extracted from images into a 3-D, vehicle-centered cartesian coordinate system aligned with the ground plane. Steering decisions are then determined in this coordinate system. A 3-D reconstruction is therefore performed before steering decisions are made.

This paper approaches the road following problem by building on the theoretical framework of the recently developed visual field theory [5, 6]. This theory provides quantitative relationships between a stationary 3-D environment and a moving camera. The theory involves pre-computing the expected instantaneous optical flow values in the camera imagery arising from every point in 3-D space.

This paper suggests that for following curved, convex roads, the tangent point on the road edge (i.e., the point on the road edge lying on an imaginary line tangent to the road edge and passing through the camera) and its optical flow are sufficient to generate control commands. Therefore, all image processing effort may be directed towards reliably finding and tracking the tangent point and extracting its optical flow.

We show how to use use the location of the tangent point (in the image) and its optical flow to generate steering wheel commands.

The control schemes presented are partial since only the kinematics of the vehicle and the camera are considered. Also, stability, robustness and sensitivity issues are not considered in this paper.

0-8194-0745-3/92/$4.00

2. DEFINITIONS AND ASSUMPTIONS

2.1 ROAD FOLLOWING

We define a *road* as any continuous, extended, curvilinear feature. The goal of road following is to follow along this feature over an extended period of time. In what we normally think of as road following, a road is defined either by its boundaries or by an extended solid or dashed white line. Here, the goal is not only to follow along these features but also to stay within a constant lateral distance from these features. Vision-based road following requires the ability to continuously detect and track features in imagery obtained from an onboard camera, and to make steering decisions based on visual properties of these features.

Figure 1 shows a point on a vehicle and the left-hand side road edge. The unit vector $\hat{h}$ is the instantaneous heading of the vehicle, O is the instantaneous center of curvature of the vehicle path, and r is the instantaneous radius of curvature of this path. We define *road following* as an activity that involves servoing $\hat{h}$ such that it follows the road edge. It is desired that $\hat{h}$ be servoed such that the vehicle is always parallel to the tangent to the local curvature of the road edge (Figure 1), and such that the distance s of a point on the vehicle from the road edge is maintained at a constant value. In other words, the instantaneous center of curvature of the road edge and the instantaneous center of curvature of the vehicle path should coincide, and the tangent to the edge of the road at the intersection point B should be parallel to $\hat{h}$. In this paper, we assume that the road is curved.

2.2 COORDINATE SYSTEM

The equations in this paper will be defined in a coordinate system which is fixed with respect to the camera on board the vehicle. This coordinate system is shown in Figure 2. We assume that the camera is mounted on a vehicle (later we explain how) moving in a stationary environment. Assume a pinhole camera model and that the pinhole point of the camera is at the origin of the coordinate system. This coordinate system is used to measure angles to points in space and to measure optical flow at these points. We use spherical coordinates (R–θ–ϕ) for this purpose. In this system, angular velocities ($\dot{\theta}$ and $\dot{\phi}$) of any point in space, say P, are identical to the optical flow values at P' in the image domain. Figure 3 illustrates this concept: θ and ϕ of a point in space are the same as θ and ϕ of the projected point P' in the image domain, and therefore there is no need to convert angular velocities of points in 3D space to optical flow. In Figure 3 the image domain is a sphere. However, for practical purposes the surface of the image sphere can be mapped onto an image plane (or other surface).

2.3 TWO-WHEELED VEHICLE

In this paper, we use a theoretical two-wheeled vehicle as illustrated in Figure 4. A rigid frame of length $2m$ holds both wheels. A steering wheel angle is applied to both wheels simultaneously, i.e., if one wheel is rotated by an angle β relative to the frame, the other wheel will rotate by the same angle. This apparatus assures that both wheels will always stay at the same distance from the instantaneous center of curvature of the vehicle's path. The camera is mounted such that its pinhole point is located above the front wheel center, and it rotates with the front wheel. The optical axis of the camera coincides with the instantaneous translation vector (heading) of the front wheel.

The following geometrical relationship holds for the vehicle in Figure 4:

$$r = \frac{m}{\sin\beta} \tag{1}$$

The frame length m is usually known. Thus the instantaneous radius of curvature r of the vehicle path can be determined by measuring the steering angle β.

Figure 5 is an overall description of the system including the spherical coordinate system. For convenience we chose to have the Z axis pointing down. However the same coordinate system as described in Figure 2 is used here. The camera is mounted at some height above the ground and rotates with the front wheel. The position of any point on the road can be expressed with the coordinates R, θ and ϕ, as shown in Figure 5.

In the following analysis, we assume a moving vehicle in a stationary environment. The road is assumed to be planar, and road edges are assumed to be extractable. Figure 11 shows examples of road images obtained from a camera mounted on a vehicle.

3. VISUAL FIELD THEORY

We have recently developed a new visual field theory that relates six-degree-of-freedom camera motion to optical flow for a stationary environment [5, 6]. The theory describes the structure of a field in 3-D space consisting of contours and surfaces surrounding the moving camera. The field is always centered at the camera pinhole point and moves with the camera. The structure of the field changes as a function of the instantaneous camera motion.

This theory provides us with a theoretical and scientific basis for developing constraints, control schemes, and optical flow-based visual cues for road following. This section reviews this theory as it relates to the road following problem.

3.1 EQUATIONS OF MOTION AND OPTICAL FLOW

Let the instantaneous coordinates of the point P be $\mathbf{R} = (X,Y,Z)^T$, where the superscript T denotes transpose (Figure 2). Assuming the instantaneous translational velocity of the camera is $\mathbf{t} = (U,V,W)^T$ and the instantaneous angular velocity is $\boldsymbol{\omega} = (A,B,C)^T$ then we have shown that the optical flow of point P can be expressed as [7]:

$$\begin{bmatrix} \dot{\theta} \\ \dot{\phi} \end{bmatrix} = \begin{bmatrix} \frac{-Y}{X^2+Y^2} & \frac{X}{X^2+Y^2} & 0 \\ \frac{-XZ}{\sqrt{X^2+Y^2}(X^2+Y^2+Z^2)} & \frac{-YZ}{\sqrt{X^2+Y^2}(X^2+Y^2+Z^2)} & \frac{\sqrt{X^2+Y^2}}{X^2+Y^2+Z^2} \end{bmatrix} \begin{bmatrix} -U-BZ+CY \\ -V-CX+AZ \\ -W-AY+BX \end{bmatrix} \tag{2}$$

where dot denotes first derivative with respect to time. As mentioned earlier, $\dot{\theta}$ and $\dot{\phi}$ of a point in space (i.e., the angular velocities in the camera coordinate system) are the *same* as the optical flow components $\dot{\theta}$ and $\dot{\phi}$ (Figure 3).

Suppose that we want to determine the locus of points in 3-D space that produce constant optical flow values $\dot{\theta}$ and constant optical flow values $\dot{\phi}$ in the image for a given arbitrary six-degree-of-freedom camera motion. To do so we simply set $\dot{\theta}$ and $\dot{\phi}$ in equation set (2) to the desired constants and solve for X, Y, and Z. However, the solution to these two equations is not unique since there are three unknowns and two equations. In general, there is an infinite number of solutions.

3.2 A SPECIAL CASE

In this section we analyze a specific motion in the instantaneous XY ($\phi = 0$) plane of the camera coordinate system.

Let the camera motion vectors $\mathbf{t}$ and $\boldsymbol{\omega}$ be given as follows:

$$\mathbf{t} = (U,V,0)^T \tag{3}$$

$$\boldsymbol{\omega} = (0,0,C)^T. \tag{4}$$

This means that the translation vector may lie anywhere in the instantanous XY plane while the rotation is about the Z-axis. Substituting these motion vectors into equation set (2) yields:

$$\begin{bmatrix}\dot{\theta}\\ \dot{\phi}\end{bmatrix} = \begin{bmatrix} \frac{-Y}{X^2+Y^2} & \frac{X}{X^2+Y^2} & 0 \\ \frac{-XZ}{\sqrt{X^2+Y^2}(X^2+Y^2+Z^2)} & \frac{-YZ}{\sqrt{X^2+Y^2}(X^2+Y^2+Z^2)} & \frac{\sqrt{X^2+Y^2}}{X^2+Y^2+Z^2} \end{bmatrix} \begin{bmatrix} -U+CY \\ -V-CX \\ 0 \end{bmatrix}. \quad (5)$$

Setting $\dot{\theta}$ and $\dot{\phi}$ in equation set (5) to constants will result in a set of equal flow points for this specific motion.

Consider the case where the optical flow value of $\dot{\theta}$ is constant. From equation set (5), the points in space that result from constant $\dot{\theta}$ (regardless of the value of $\dot{\phi}$) form a cylinder of infinite height whose equation is

$$\left[X+\frac{V}{2(C+\dot{\theta})}\right]^2+\left[Y-\frac{U}{2(C+\dot{\theta})}\right]^2=\left[\frac{V}{2(C+\dot{\theta})}\right]^2+\left[\frac{U}{2(C+\dot{\theta})}\right]^2, \quad (6)$$

as displayed in Figure 6.

The meaning of equation (6) is the following: all points in 3-D space that lie on the cylinder described by Equation (6) and which are visible (i.e., unoccluded and in the field of view of the camera) produce the same instantaneous horizontal optical flow $\dot{\theta}$. We call the cylinder on which equal flow points lie the *equal flow cylinder*.

3.3 ZERO FLOW CYLINDERS

One of the equal flow cylinders corresponds to points in 3-D space that produce zero horizontal flow. We call this cylinder a *zero flow cylinder*. The equation that describes the zero flow cylinder can be obtained by setting $\dot{\theta} = 0$ in Equation (6), i.e.,

$$\left[X+\frac{V}{2C}\right]^2+\left[Y-\frac{U}{2C}\right]^2=\left[\frac{V}{2C}\right]^2+\left[\frac{U}{2C}\right]^2. \quad (7)$$

We have shown [5] that if the Z component of the camera rotation vector ω is positive (i.e., $C > 0$), then visible points in the XY plane that are inside the zero flow cylinder produce positive horizontal optical flow ($\dot{\theta} > 0$), while visible points outside the zero flow cylinder produce negative horizontal optical flow ($\dot{\theta} < 0$) in the image (see Figure 7). If ω is negative (i.e., $C > 0$) then the opposite is true.

3.4 EQUAL FLOW CYLINDERS AS A FUNCTION OF TIME

As the camera moves through 3-D space, the equal flow cylinders move with it. Figure 8 shows sections of equal flow cylinders as a function of time. At each instant of time, the radii of the equal flow cylinders are a function of the instantaneous motion parameters t and ω. The locations of the equal flow cylinders are such that they always contain the origin of the camera coordinate system (the same as the camera pinhole point), are tangent to the instantaneous translation vector t, and their symmetry axes are parallel to the instantaneous rotation vector ω. (In Figure 8, the direction of ω varies over time.) Each zero flow cylinder lies to the left or right of the translation vector depending on whether the instantanous rotation is positive or negative, respectively.

4. ANALYSIS OF ROAD FOLLOWING

We describe two road following scenarios. The first one is for a circular road, where we outline basic geometric and motion-related relationships. Using this relatively simple case, we explain the problem of following a road using a vision sensor, problems associated with it, and relate it to the visual field theory described above. We also suggest road following control approaches. The second road following scenario is for an arbitrary convex curved road, where we also suggest control approaches.

4.1 CIRCULAR ROAD

In this section, we consider following along a circular road. Given visual cues, a goal of a control system is to find the steering angle. If the vehicle is already on a path that follows the road, then only *changes* in steering angle are necessary. Figure 9 shows a vehicle moving around a circular road of radius l. The path traversed by the vehicle is a circle of radius r. Let the unit vector $\hat{t}$ indicate the direction of the *tangent line,* a line that contains the camera pinhole point and is tangent to the road edge.

It can be proved [7] that the tangent point T lies on the instantaneous zero flow cylinder if the camera orientation is fixed relative to the vehicle. This proof holds no matter what the diameter of the circular road edge. This means that no matter how far the vehicle is from the road edge (Figures 10 and 11a), the tangent point lies on the zero flow cylinder. Thus the horizontal component of optical flow of the tangent point is always zero.

In Figure 9, therefore, the optical flow $\dot{\theta}$ due to point T is zero. Let the distance from the vehicle to the road edge be s, and let θ be the positive angle to $\hat{t}$ measured from the X-axis. From Figure 9, the following relationships hold:

$$l = r \sin\theta \tag{8}$$

$$s = r - l = r(1-\sin\theta) \tag{9}$$

Differentiating Equation (8) with respect to time:

$$\dot{l} = \dot{r}\sin\theta + r\dot{\theta}\cos\theta \tag{10}$$

where dot denotes derivative with respect to time. For a circular road, l is constant, and thus $\dot{l}$ can be set to zero in Equation (10):

$$0 = \dot{r}\sin\theta + r\dot{\theta}\cos\theta$$

$$\dot{r} = -r\,\dot{\theta}\,cot\,\theta \tag{11}$$

When the vehicle is moving on a perfect circular path both $\dot{r}$ and $\dot{\theta}$ are equal to zero. However, suppose the vehicle's path is not a perfect circle. Since r is the instantaneous radius of curvature of the vehicle motion, $\dot{r}$ is the rate at which the curvature changes. Equation (11) suggests a way of controlling the vehicle motion so as to achieve a constant circular motion. Consider the two-wheeled vehicle described in Section 2.3. From Equation (1), we can derive the following:

$$\beta = \sin^{-1}(\frac{m}{r}). \tag{12}$$

Equation (12) gives a value of the steering angle β as a function of the instantaneous radius of curvature r and the distance $2m$ between the two wheels. Normally the value m is known. For a more realistic vehicle (such as a four-wheeled vehicle with front-wheel steering), some other relationship may hold.

In Equation (11), $\dot{r}$ is the rate at which the radius of curvature of the vehicle motion is changing. We can express $\dot{r}$ as a function of the steering angle β by differentiating Equation (1) with respect to time:

$$\dot{r} = \frac{-m\cos\beta}{\sin^2\beta}\,\dot{\beta} \tag{13}$$

Substituting Equations (13) and (1) into (11) and solving for $\dot{\beta}$:

$$\dot{\beta} = \dot{\theta}\tan\beta\,cot\,\theta \tag{14}$$

Equation (14) suggests a partial control scheme whose inputs are the current steering angle β, the current angle θ of the tangent line relative to the X-axis, and the optical flow $\dot{\theta}$ of the tangent point. All of these inputs can be measured. The variable being computed is the rate of change of the steering angle, $\dot{\beta}$. Equation (14) provides the gain $\tan\beta cot\,\theta$ by which $\dot{\theta}$ should be multiplied in

order to get the correct change in steering wheel angle. This gain depends on the current steering wheel angle β and the angular location θ of the tangent point in the image.

Figure 11b shows a sequence of images taken from a camera mounted on a vehicle. The images in the figure are numbered in the same order in which they were taken. The road is almost circular. Note that the tangent point (almost) stays at the same location in each image in the sequence. If the road were perfectly circular and the vehicle were moving on a perfect circular path, then the position of the tangent point would not change from image to image. However, if the vehicle's path is not a perfect circle, then its steering can be controlled by measuring horizontal changes in the position of the tangent point. These changes are the horizontal component of optical flow at that point, and can be used to generate changes ($\dot{\beta}$) in the steering wheel command β.

It is important to emphasize that the derivation of $\dot{\beta}$ takes into account the kinematics of the system but *not* the dynamics. This is also the reason why we emphasize that the control scheme is not complete.

If the rate of change of the steering angle, $\dot{\beta}$, is the only variable being controlled (as indicated in Equation (14)), then in practice the vehicle may not maintain a constant distance from the edge of the road. Therefore, in addition to Equation (14), Equation (9) can also be used to control the vehicle to achieve a constant circular motion. Substituting Equation (1) into (9):

$$s = \frac{m}{\sin\beta}(1-\sin\theta)$$

or

$$\beta = \sin^{-1}[\frac{m}{s}(1-\sin\theta)] \tag{15}$$

Equation (15) suggests a partial control scheme whose inputs are the measured angle θ of the tangent line relative to the X-axis, the desired distance s of the vehicle from the road edge, and the distance $2m$ between the front and rear wheels. The variable being computed is the steering angle β.

The control signals (β and $\dot{\beta}$) and partial control schemes suggested above assume that the road is circular, that the center of curvature of the vehicle path coincides with the center of curvature of the circular road, and that the road is planar. It is also assumed that the tangent point (in the image) is traceable, and that the vehicle heading coincides with the camera optical axis. There are several advantages to this approach: (1) it is simple and therefore computationally inexpensive, (2) it is independent of the speed of the vehicle, (3) it is independent of the camera height above the road, (4) only a few measurements are necessary to control the vehicle, and (5) only a very small portion of the image -- the portion around the tangent point -- needs to be analyzed, in principle. (Of course, item (5) may not be true in practice since larger portions of the road may have to be extracted in order to reliably find the tangent point.)

4.2 CURVED ROAD FOLLOWING

In this section, we consider road following for the case where the curvature of a convex road is not constant. Figure 12 shows two cases. In Figure 12a the radius of curvature increases as the vehicle moves. In Figure 12b, the radius of curvature decreases. In Figure 12a, let the current instantaneous center of curvature of the vehicle path be at O. If the road curvature were constant (indicated by an imaginary road shown as a dotted line in Figure 12a), then the point of tangency of the vector $\hat{t}$ would lie on this imaginary road, and this point would lie on the zero flow cylinder. However, because the road's curvature is changing, the point of tangency is at T. Notice that the point T lies on some equal flow cylinder whose θ optical flow is negative (T lies outside the zero flow cylinder). If the radius of curvature were decreasing (Figure 12b), the tangent point would lie inside the zero flow cylinder, and its θ optical flow would be positive. Therefore, intuitively, if the horizontal component of the optical flow, $\dot{\theta}$, at the tangent point is measured, then its value can be used as a control signal for steering the vehicle. If $\dot{\theta}$ is negative (Figure 12a) then the

steering command is to increase the radius of curvature of the vehicle's current motion. If $\dot{\theta}$ is positive (Figure 12b), then the steering command is to decrease the radius of curvature of the vehicle's current motion by sharpening the turn.

5. CONCLUSION

In this paper, we have shown that, in principle, a road feature sufficient for following curved, convex roads is the location of the tangent point on the road edge as projected on the image and its optical flow. In practice, larger portions of the road may have to be extracted in order to reliably find the tangent point. We also showed that fast, simple control approaches are possible that directly use measured image quantities.

The partial control schemes presented in this paper have not been implemented yet. Current and future work will be directed towards implementing control algorithms that use the approaches suggested in this paper [11]. Issues such as the dynamics of the vehicle, sensitivity, stability, robustness, and time delays must be considered when developing control algorithms for real vehicles.

6. REFERENCES

1. Aloimonos, J. "Purposive and Qualitative Active Vision." *Proc. DARPA Image Understanding Workshop,* September 1990.
2. Crisman, J. and Thorpe, C. "Color Vision for Road Following." *Vision and Navigation: The Carnegie Mellon Navlab.* Kluwer Academic Publishers, 1990, Chapter 2.
3. Dickmans, E. and Grafe, V. "Applications of Dynamic Monocular Machine Vision." *Machine Vision and Applications,* Vol. 1, 1988.
4. Dickmans, E. and Grafe, V. "Dynamic Monocular Machine Vision." *Machine Vision and Applications,* Vol. 1, 1988.
5. Raviv, D. "A Quantitative Approach to Camera Fixation." *Proc. IEEE Conf. on Computer Vision and Pattern Recognition,* Maui, Hawaii, June 1991.
6. Raviv, D. and Herman, M. "Towards an Understanding of Camera Fixation." *Proc. 1990 IEEE International Conference on Robotics and Automation,* Cincinnati, Ohio, May 1990, 28-33.
7. Raviv, D. and Herman, M. "A New Approach to Vision and Control for Road Following." Internal Report NISTIR 4476, National Institute of Standards and Technology, January 1991.
8. Thorpe, C., Hebert, M., Kanade, T. and Shafer, S. "Vision and Navigation for the Carnegie-Mellon Navlab." *IEEE Trans. on Pattern Analysis and Machine Intelligence,* 10(3), 1988.
9. Turk, M., Morgenthaler, D., Gremban, K. and Marra, M. "VITS -- A Vision System for Autonomous Land Vehicle Navigation." *IEEE Trans. on Pattern Analysis and Machine Intelligence,* May 1988.
10. Waxman, A., LeMoigne, J., Davis, L. and Siddalingalah, T. "A Visual Navigation System for Autonomous Land Vehicle." *IEEE Journal Robotics and Automation,* RA-3:124-141, April 1987.
11. Yakali, H. H., Raviv, D. and Herman, M. "Road Following - A New Approach." *Proc. Fourth Conference on Recent Advances in Robotics,* Florida Atlantic University, Boca Raton, Florida, May 1991.

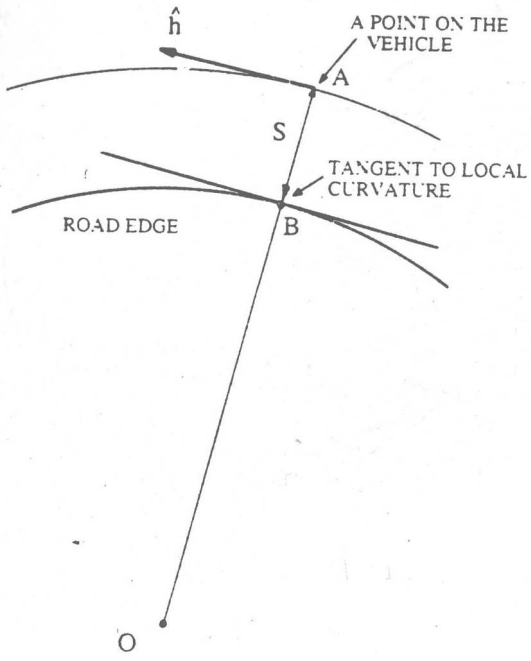

Figure 1. Road following.

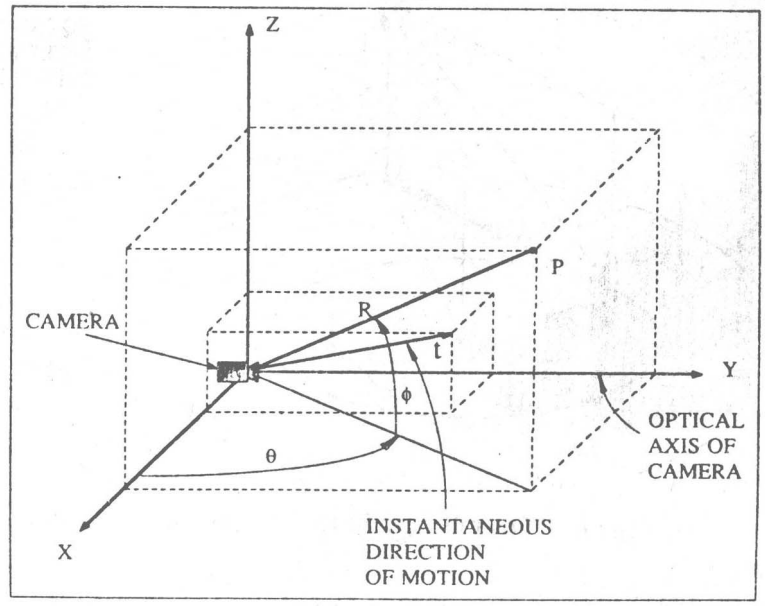

Figure 2. Coordinate system fixed to camera.

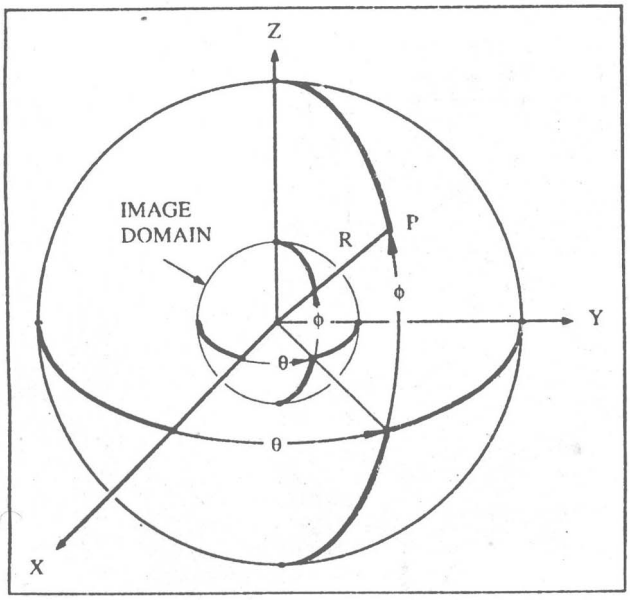

Figure 3. Image domain.

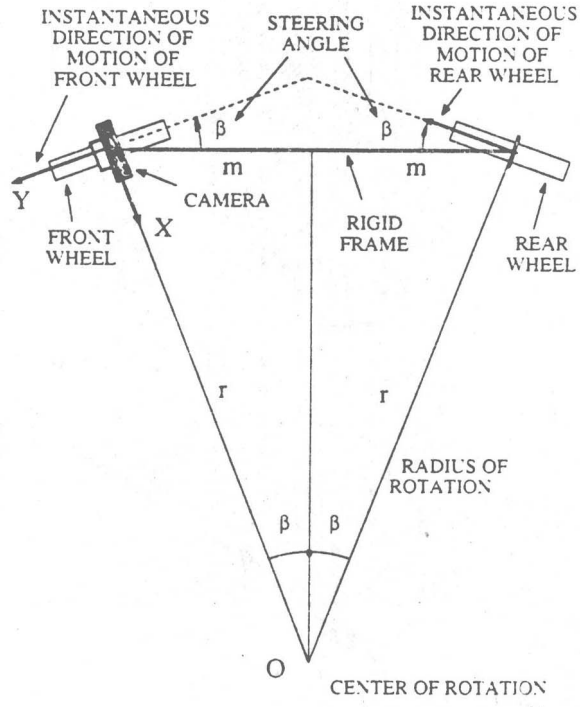

Figure 4. Two-wheeled vehicle with camera.